Tungsten Fiber Reinforced Tungsten (W_f/W) using Yarn Based Textile Preforms

J.W.Coenen[a,*],P.Huber[d],A. Lau[a] ,L.Raumann[a], D.Schwalenberg[a], Y.Mao[a], J.Riesch[b], A.Terra[a], Ch.Linsmeier[a], R.Neu[b,c]

[a]Forschungszentrum Jülich GmbH, Institut für Energie- und Klimaforschung 52425 Jülich, Germany
[b]Max-Planck-Institut für Plasmaphysik, 85748 Garching, Germany
[c]Technische Universität München, 85748 Garching, Germany
[d]Institut für Textiltechnik (ITA) der RWTH Aachen University, 52074 Aachen, Germany

E-mail: j.w.coenen@fz-juelich.de

Abstract. Material related limitations are one of the main challenges for the design of future fusion reactors. Tungsten (W) as the primary material choice is considered resilient against erosion, has the highest melting point of any metal and shows low activation after neutron irradiation. However, W is intrinsically brittle and faces operational embrittlement. To overcome these issues, W-based composites have been in development. W fiber-reinforced W composite materials (W_f/W) incorporate extrinsic toughening mechanisms allowing the redistribution of stress peaks and thus overcoming the intrinsic brittleness problem.

In this contribution recent results on the incorporation of new textile preformes into W_f/W production will be given with a focus on the production via chemical vapor deposition of tungsten-based materials. The use of tungsten yarns, instead of single wires for the textile production is elaborated.

1. Introduction

Bulk tungsten (W) components are typically considered as the main candidate for plasma-facing comnpoents in the highly loaded divertor of existing and planned fusion reactors. Tungsten has a very low sputtering yield, the highest melting point of any metal, and behaves relatively well in terms of its properties after neutron irradiation. With respect to the interaction with the fusion fuel, tungsten shows low retention of hydrogen isotopes including tritium.

Many current studies have addressed the issues related to qualify materials for ITER ‡ [1–4] and beyond. For the next step e.g. a Demonstration Reactor (DEMO),§ the imposed limits for materials and components will be extremely challenging. Many of

‡ https://www.iter.org
§ https://www.euro-fusion.org/programme/demo/

the boundary conditions [5,6] to be imposed for the materials will be above the technical feasibility limits as they are set out today [3, 7].

New concepts for plasma-facing components (PFCs) are being studied (see [2, 8], and references therein) concentrating on crack resilient materials with low activation, small or no fuel retention, extended lifetime with respect to low erosion and brittle failure.

In this contribution the focus lies on the use of multifilament tungsten yarns, a concept introduced in [9]. These can play a major role in improving the behavior of tungsten fiber-reinforced tungsten W_f/W, cf section 2.

While previously only the different yarn types were elaborated, this paper concentrates on the production of tungsten yarns (section 3), the introduction into weaves(section 4), and the subsequent initial experiments on the introduction of yarn based weaves into a single layer of W-CVD matrix (section 5). In effect it is an attempt to evaluate the possibility of utilising multifilament yarns as base material for the production of high density CVD W_f/W with introducing high strength filaments.

2. Tungsten Fiber-Reinforced Tungsten

2.1. Composite Approach

To overcome the brittleness of W a W fiber-reinforced W composite material (W_f/W), incorporating extrinsic toughening mechanisms as described in [8,10] is being developed.

The basic concept of materials such as W_f/W makes use of a composite approach.

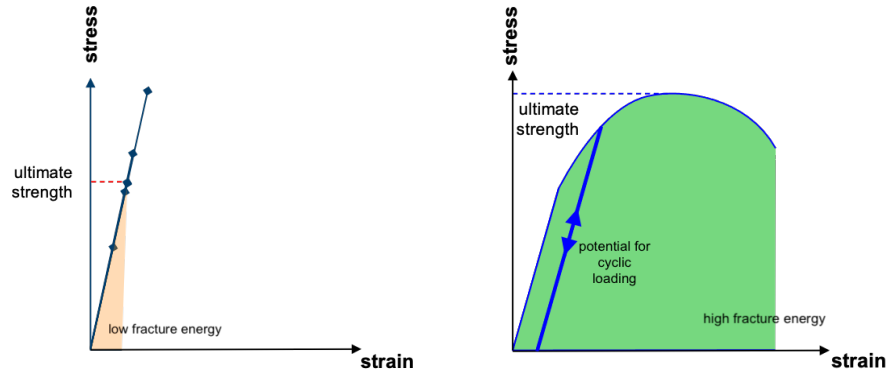

(a) Brittle material - Points represent statistically varying UTS

(b) Ductile / Tough Material

Figure 1: Schematic view of the typical stress-strain behaviour for a material, e.g. tungsten, when being brittle or ductile (tough)

Figure 1 visualises the issue of brittle materials, e.g. with tungsten. In 1(a), the stress-strain curve for a fully brittle material is shown. Failure occurs in a sudden

manner, immediately when the Ultimate Tensile Strength (UTS) is reached. UTS here is statistically distributed and not well defined as it is determined by the weakest point in the material (Weibull statistics).

In 1(b), a material is shown with well defined material properties, with high toughness and ductility. The shown material is intrinsically failure tolerant, with no sudden failure and remains load bearing, beyond UTS, also allowing cyclic loading of the material.

In order to improve the mechanical properties of brittle materials such as W several options had been considered: microstructural refinement, alloying or composites [11–17]. Here we are briefly summarizing the W_f/W.

2.2. Brief introduction on W_f/W

Productions methods for W_f/W composites do include, either Chemical Vapor Deposition (CVD) [18, 19] or powder metallurgical (PM) processes [20–24]. Both methods are able to produce a high density composite.

The chemical vapour deposition of tungsten was frequently used for the production of W_f/W as it allows low processing temperatures and a force-free production. The used process is the heterogeneous surface reaction of WF_6 and H_2 to form a solid W deposit and gaseous HF. This process is highly sensitive to the partial pressures as well as temperatures and the details are given in [25–27]

In recent times both processes have been scaled to allow larger production as shown in figure 2. The examples shown are two W_f/W discs based on a short fiber composite utilising 2.4mm short W fibers.

(a) Powder metallurgically produced W_f/W produced similar to the process as depicted in [20, 22]

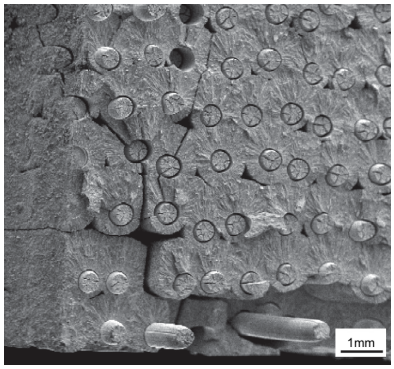

(b) SEM micrograph of a fracture surface of CVD W_f/W (based on [28]) showing both the CVD matrix as well as the unidirectional fibers

Figure 2: Example of PM W_f/W bulk material (a) as well as a typical fracture surface of long-fiber CVD W_f/W (b)

Based on existing work [28–34], the basic proof-of-principle for both W_f/W

materials (PM and CVD Wf/W) was given. The typical construction of the composite is based on wires, coated with an oxide ceramic e.g. Y_2O_3 and a W-matrix. The interface is the main vehicle to enable pseudo-ductile behavior.

W_f/W shows pseudo-ductile behaviour even at room temperature for both the PM and CVD routes. This means despite crack formation, load bearing capability is retained.

One of the main aims for W_f/W when optimising the production process is to retain as many of the beneficial material properties of the constituents as possible. It is crucial to allow for optimal extrinsic toughening and pseudo-ductility. Here in particular the properties of the used wires and filaments are essential.

The interplay between the interface and the strength of the fiber as well as the preform [30] are important for beneficial material properties. Here Yttria is an ideal candidate as interface material for the W_f/W composite due to its several advantageous properties: good thermal and chemical stability, high mechanical strength and hardness [35, 36] as well as low neutron activation. To improve the CVD W_f/W material multiple avenues are being pursued including CVD parameter optimisation [25–27]. Here improving the textile preform as well as improving the CVD matrix production are among the most promising ones.

2.3. Overview on Wires and Weaves

For the use in W_f/W potassium doped W-wires are used as they essentially minimise the temperature induced embrittlement and as such allow the fibers or filaments to retain their ductility even after exposure to high temperatures (above 1500 K) [28]. The toughening mechanism that is directly linked to this behaviour is the ductile fiber deformation [37, 38]. Properties of the fibers can however be degraded by various circumstances e.g. by impurities during fabrication [39, 40], high-temperatures or neutron irradiation during operation [41, 42].

For optimised W_f/W material properties tungsten preforms with advanced fiber types e.g. yarns can contribute by introducing better properties e.g. tensile strength at the point of production. From previous work it is known that the strength of the $16\,\mu m$ filament is at $4500\,MPa$ significantly higher than the strength of the $150\,\mu m$ fiber ($\sim$2500 MPa) (in the as-fabricated state) [9, 30].

In the past, monofilaments with a diameter of $150\,\mu m$ (OSRAM) have been used to weave textile preforms to facilitate large scale CVD W_f/W production [10, 30]. During the CVD process, the improvement of the W_f/W properties can be realised by optimising the process parameters, optimal fiber sizing (interface), and fiber positioning, with respect to fiber volume fraction, relative density, and WF_6 consumption [27].

However, the high stiffness of the woven tungsten fabric with $150\,\mu m$ diameter often presents some challenges, i.e. positioning of a flat preform during the CVD processes. In Figure 3, a typical weave produced from $150\,\mu m$ wire is shown. In order to improve these textile performs or weaves more flexible $16\,\mu m$ or $25\,\mu m$ fibers can be used. Here

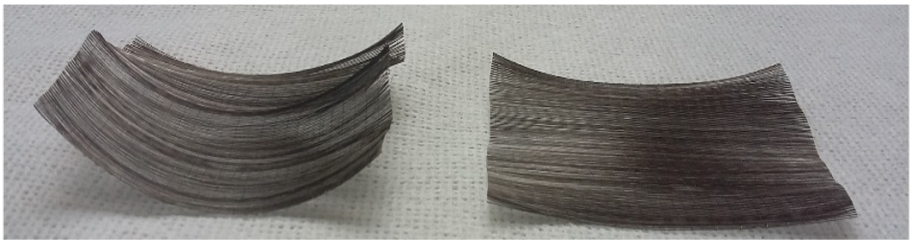

Figure 3: Tungsten weave based on production described in [30] - The weaves are 55-60mm wide

the production of tungsten yarns as proposed in [9] and weaves as proposed can help.

3. Tungsten Yarn

In order to optimise the production of textile preforms by improving the more flexible and strong filaments yarns are being used. Here the benefit lies in the use of yarns to cohesively introduce the filaments in a way not to be limited by the small dimensions of the yarns during handling. Based on [9] braided yarns were selected.

Braided yarns are based on a very versatile textile process, that offers various possible variation of the braid and the machine itself. Only the process of radial braiding is relevant for the work presented. Based on the process shown in 4(a) and the selection made in [9] the following yarn type is considered here: Triaxial braided yarns with overbraiding of core filaments (16 + 7 Filaments) (see Fig. 4(b)). The filaments were supplied by OSRAM, similar to the weft wire for weaving and the original 150 micron wire used in the conventional W_f/W.

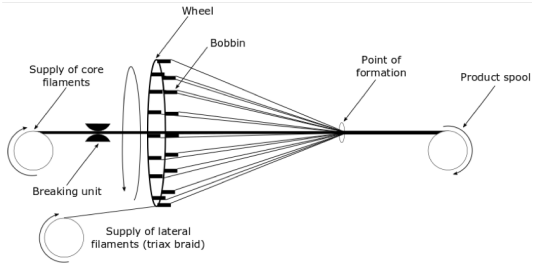

(a) Principle of braiding [9]

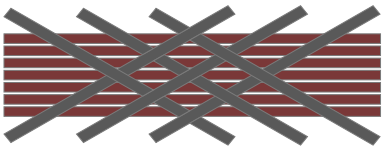

(b) Triaxial braid: sleeve filaments (black) and non-interlaced core filaments (red)

Figure 4: Procedures (a) and braiding (b) based on [9]

After the initial success in yarn production a larger amount of triaxial braided yarn with core filaments were industrially produced and used for weaving of advanced preforms. The braided yarn structures were fabricated based on the study in and manufactured by Bossert&Kast GmbH + Co. KG. 16 carriers were used and the braid pattern was selected to "one over two, under two". For details see [9].

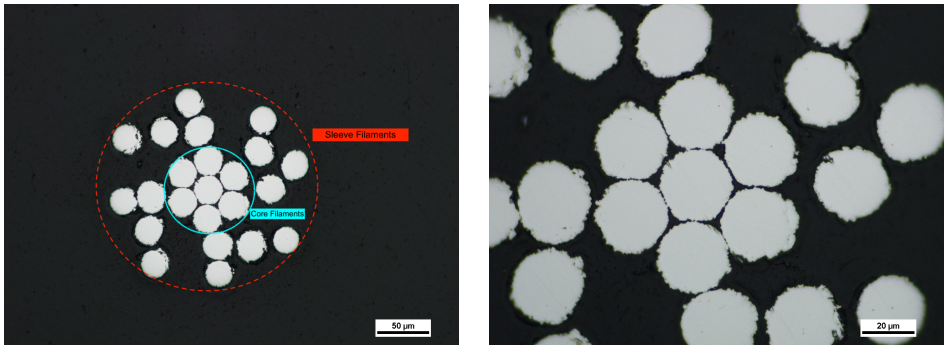

(a) (b)

Figure 5: Structures of the individual yarns, showing both the cores and the sleeve filaments. Image has been produced by optical emission light microscope (Zeiss Axios Observer Z)

In contrast to the previous study $25\mu m$ filaments were used (cf Fig. 5) as the acting forces during the braiding process otherwise too many filaments were torn during production. The yarns structure otherwise is identical to the ones presented in [9]. The diameter of the yarns produced is around $195\mu m$. The diameter being the envelop of the outermost filaments in the case of the braided yarn.

4. Tungsten Weave

The above described yarns are then woven similarly to the conventional process using a single wire. The superior weavability of the yarn allows a much more flexible textile preform to be manufactured, which in turn allows better placement during the production process. Here two types of weaves are being compared: A weave with the warp wire made from yarns and a classical $50\,\mu m$ tungsten filament in the weft direction and a second one utilising the identical yarn type in both warp and weft direction. Both weaves were based on the triaxial braid with 16 filaments + 7 core filaments.

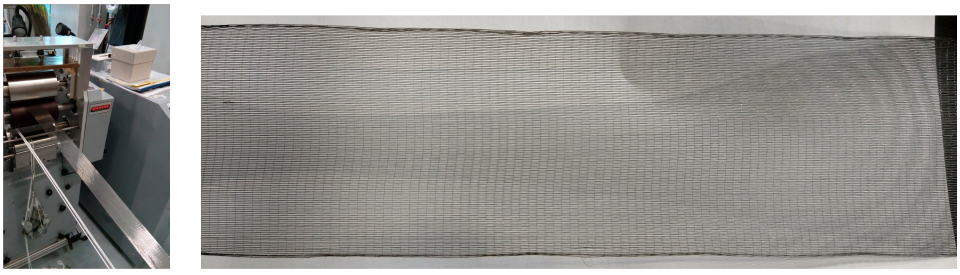

(a) (b)

Figure 6: Fotograph of a Mageba shuttle loom (type SL 1/80) during weaving (a) and final weave (55mm wide) (b)

A Mageba shuttle loom (type SL 1/80) ‖ weaving machine figure 6(a) was used to produce the weaves figure 6(b). The reed used for weaving has 21.7 dents per cm and a width of 60.5 mm, this lead to a total of 130 weft wires. This means the centre of each yarn is 460μm apart from the next. Both weaves show a good quality with some obvious differences in structure (Fig. 7).

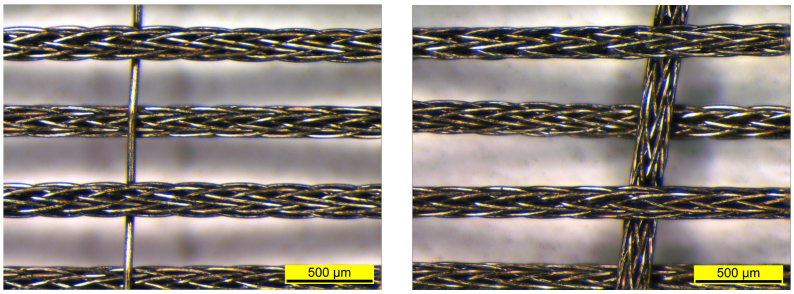

(a) Weave 1 based on yarn and 50μm weft wire

(b) Weave 2 based on yarn weft and warp

Figure 7: Tungsten weaves (see section 4) produced based on the braided tungsten yarn as described in section 3 - Images obtained via Zeiss optical microscope

While the weave with a single weft wire (weave 1) is relatively thin (350μm) (Fig. 8(a)), the yarn only weave is almost 600 μm in thickness (Fig. 8(b)). In order to

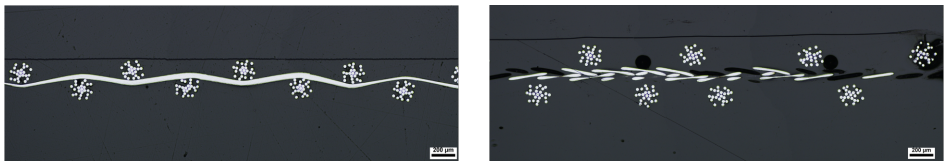

(a) Weave based on yarn and 50μm weft wire

(b) Weave based on yarn weft and warp

Figure 8: Metallgraphic cuts through textile preforms - two types of weaves (images made with Nikon Eclipse LV 150 NL).

optimise the CVD process these differences will play a role in order to mitigate porosity.

5. W-Weaves with CVD Tungsten Matrix

Tungsten weaves based on single wire (150 μm) are currently the standard way of introducing unidirectional tungsten fibers into the CVD tungsten matrix. Based on the optimisation weaving process developed in [30] weaves are prepared on the same Mageba shuttle loom (type SL 1/80) weaving machine and then introduced in the CVD reactor [25]. This results in layers with slightly undulating positions of the wires, due to the introduction of a 50 μm weft wire. In figure 9 the bottom layer of a CVD W_f/W composite is shown.

‖ Mageba International GmbH, Bernkastel, Germany

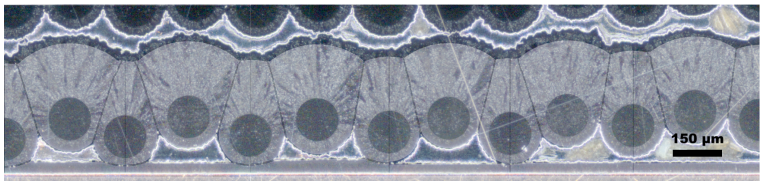

Figure 9: Bottom layer of CVD W_f/W based on figure in [25], the picture shows an image via optical microscopy - white overlays highlight the simulated growth of CVD W on the individual fibers.

In figure 9 also the growth of the CVD matrix is highlighted by an overlay of the different section / direction of the grain-growth. Based on the results attained in [25–27] it can be surmised that with optimised CVD process parameters all surfaces can be coated with CVD W at a nearly identical rate. Thus the matrix grows together and forms pores defined by the dimension and spacing of the wires. Figure 9 shows the typical structure that can be achieved. (For details refer to [25–27]) As a first estimate it can be deduced that the optimal distance to minimise pores and maximise density is defined by a spacing between the fibers that is at least equal to twice the fiber radius or slightly larger. This is in consequence the reason that for the use of yarns the weaving distance needs to be adapted based on the slightly larger radius of 195 μm fiber.

In figure 10 the very first CVD coating on yarn based W-weaves is shown. The coating was performed at a temperature of $500°C$, and a pressure of 130mbar.

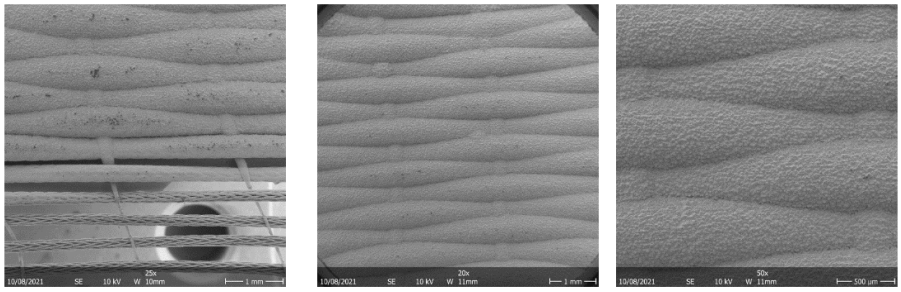

(a)

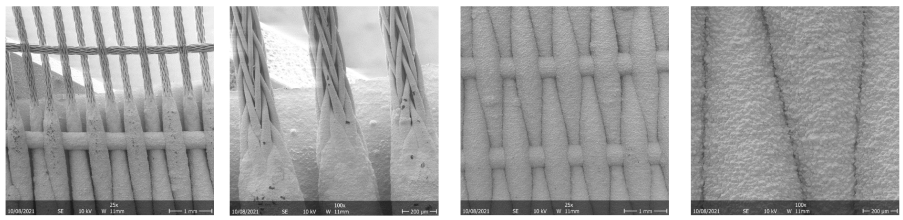

(b)

Figure 10: Tungsten weaves (see section 4) produced based on the braided tungsten yarn as described in section 3 - Images obtained via a Carl Zeiss LEO DSM 982 (a) is based on weave 1 and (b) on weave 2

For both types of weaves (cf figure 7) a dense coating was achieved filling the gaps between the individual wires with no visible defects. At the edge of the heated zone a transition between the coated and non coated yarns is observed giving an initial insight into the issues related to the used of yarns. Figure 10 shows the view onto the coated surface with the yarns now incorporated into the tungsten matrix. As stated above and in more details described in [25–27] one expected the CVD matrix to grow evenly on all surfaces with identical temperatures. For individual wires a picture as in figure 9 is produced. For a yarn containing as in this case 16+7 filaments each surface has to be considered individually and thus pores can be expected. In figure 11 a cut through

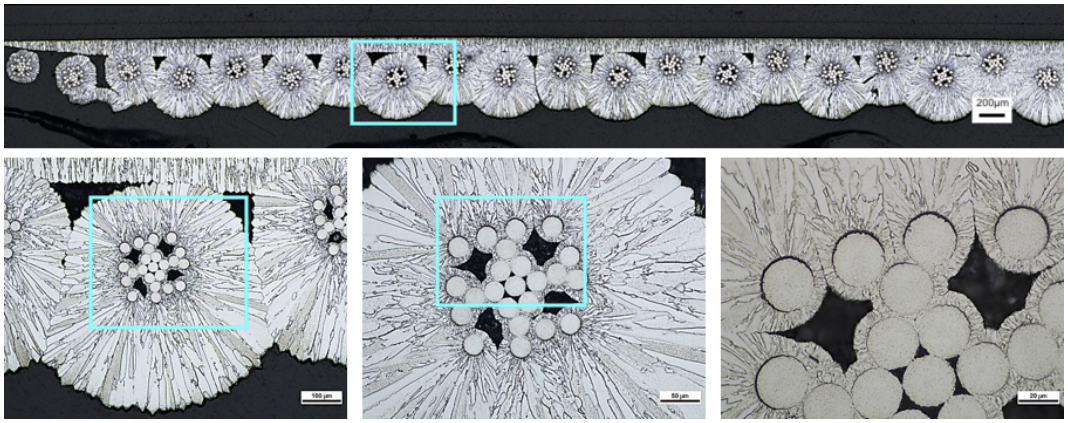

Figure 11: Bottom Layer of a yarn based CVD W_f/W after the coating process. Weave is similar to the one shown in figure 7(a), At the top a cut through part of the layer is shown, where as higher magnifications are shown at the bottom. The images were taken with a Zeiss Axio Observer Z optical microscope.

one of the coated yarn based weaves is shown. Clearly one can see the CVD matrix growing away from the individual filaments as well as the yarn as a whole. Very clearly the above descirbed effect is visible where as soon as the gap between the individual wires or filaments is closed, no further matrix can be deposited due to lack of access for the precursors. For a yarn based CVD W_f/W this means that even though the spacing between the yarns can be optimised, some porosity within the yarn will remain. Here only the optimisation of the yarn structure will help. Overall the layer of yarn based CVD W_f/W shows a good adhesion to the heated surface, even grain growth and low porosity. Further tests on multilayer yarn based CVD W_f/W are in preparation to evaluate the overall ability to produce a composite structure with enhanced properties compared to the conventional single fiber material.

In figure 11 one can also identify a small interlayer between matrix and filaments. This interlayer or interface is the aforementioned Y_2O_3. Coated in an in-house PVD process via magnetron sputtering [36] the coating can enable the pseudo-ductile behaviour. As the PVD process is line-of-sight based one can see that only the outer edges are coated, as seen in figure 11 and figure 12. In how far this will effect the composite behaviour is subject to further multilayer experiments including mechanical

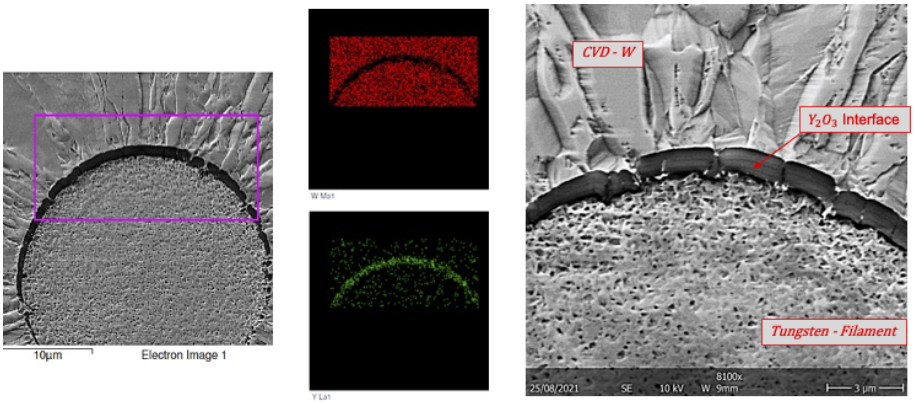

Figure 12: SEM micrograph of the region surrounding a single filament showing from left to right the overview of the filament and matrix, the W and Yttrium signals from electron diffraction as well as close up view of the microstructure.

testing.

6. Summary & Outlook

In summary it can be stated that for the first time textile preforms for W_f/W utilising yarns were produced and these weaves were then successfully used for initial single layer CVD W_f/W production. The yarns are an industrial product and are available for further studies. Similarly the weave is based on a standardised technique thus also here good quality was reached as shown in section 4.

Based on the work stated section 5 we know that in order to reach a fully dense material the ratio of distance between the individual wires must be at least as large as the distance between the individual layers during production, as otherwise the restricted gas flow will be resulting in increased porosity. These distance chosen here conforms to that measure and it is deomnstrated that at least a single layer can be produced with good quality and even growth. The only observed porosity here is related to the filament structure of the yarn, which can at this stage not be overcome. Further testing of these weaves in the CVD (W_f/W) production, in particular for multilayer composites is thus essential to study the density and fiber volume fraction, as well as the derived mechanical and thermal properties. These results open up the path towards CVD W_f/W with a much better layer placement, better density, and due to the superior filament strength also a material with better mechanical properties. The next step in production will be a 5 layer composite to produce small scale samples for 3 point bending tests.

Acknowledgements

The authors would like to thank Erika Barcan for producing the fabrics as well as her commitment to optimising the weaving parameters and the use of the material. We would also like to thank Beatrix Goeth for here work on the micrographs.

This work has been carried out within the framework of the EUROfusion. Consortium and has received funding from the Euratom research and training programme 2014-2018 and 2019-2020 under grant agreement No 633053. The views and opinions expressed herein do not necessarily reflect those of the European Commission

[1] R.A. Pitts, S. Carpentier, F. Escourbiac, T. Hirai, V. Komarov, S. Lisgo, A.S. Kukushkin, A. Loarte, M. Merola, A. Sashala Naik, R. Mitteau, M. Sugihara, B. Bazylev, and P.C. Stangeby. A full tungsten divertor for ITEr: physics issues and design status. *Journal of Nuclear Materials*, 438:S48, 2013.

[2] Ch. Linsmeier, M. Rieth, J. Aktaa, T. Chikada, A. Hoffmann, J. Hoffmann, A. Houben, H. Kurishita, X. Jin, M. Li, A. Litnovsky, S. Matsuo, A. von Müller, V. Nikolic, T. Palacios, R. Pippan, D. Qu, J. Reiser, J. Riesch, T. Shikama, R. Stieglitz, T. Weber, S. Wurster, J.-H. You, and Z. Zhou. Development of advanced high heat flux and plasma-facing materials. *Nuclear Fusion*, 57(9):092007, jun 2017.

[3] V. Philipps. Tungsten as material for plasma-facing components in fusion devices. *Journal of Nuclear Materials*, 415(1):2–9, 2011.

[4] Y. Ueda, K. Schmid, M. Balden, W. Coenen J., T. Loewenhoff, A. Ito, A. Hasegawa, c. Hardie, M. Porton, and M. Gilbert. Baseline high heat flux and plasma facing materials for fusion. *Nuclear Fusion*, 57(9):092006, jun 2017.

[5] J.H. You, E. Visca, T. Barrett, B. Böswirth, F. Crescenzi, F. Domptail, M. Fursdon, F. Gallay, B-E. Ghidersa, H. Greuner, M. Li, A.v. Müller, J. Reiser, M. Richou, S. Roccella, and Ch. Vorpahl. European divertor target concepts for DEMO: Design rationales and high heat flux performance. *Nuclear Materials and Energy*, 16:1–11, aug 2018.

[6] Christian Bachmann, G. Aiello, R. Albanese, R. Ambrosino, F. Arbeiter, J. Aubert, L. Boccaccini, D. Carloni, G. Federici, U. Fischer, M. Kovari, A. Li Puma, A. Loving, I. Maione, M. Mattei, G. Mazzone, B. Meszaros, I. Palermo, P. Pereslavtsev, V. Riccardo, P. Sardain, N. Taylor, S. Villari, Z. Vizvary, A. Vaccaro, E. Visca, and R. Wenninger. Initial {DEMO} tokamak design configuration studies. *Fusion Engineering and Design*, 98-99:1423–1426, October 2015.

[7] JW Coenen, S Antusch, M Aumann, W Biel, J Du, J Engels, S Heuer, A Houben, T Hoeschen, B Jasper, et al. Materials for DEMO and reactor applications—boundary conditions and new concepts. *Physica Scripta*, 2016(T167):014002, dec 2016.

[8] J. W. Coenen. Fusion materials development at forschungszentrum juelich. *Advanced Engineering Materials*, mar 2020.

[9] J W Coenen, M Treitz, H Gietl, P Huber, T Hoeschen, L Raumann, D Schwalenberg, Y Mao, J Riesch, A Terra, Ch Broeckmann, O Guillon, Ch Linsmeier, and R Neu. The use of tungsten yarns in the production for w f /w. *Physica Scripta*, T171:014061, jan 2020.

[10] H. Gietl, S. Olbrich, J. Riesch, G. Holzner, T. Höschen, J.W. Coenen, and R. Neu. Estimation of the fracture toughness of tungsten fibre-reinforced tungsten composites. *Engineering Fracture Mechanics*, page 107011, apr 2020.

[11] Lauren M Garrison, Yutai Katoh, Lance L Snead, Thak Sang Byun, Jens Reiser, and Michael Rieth. Irradiation effects in tungsten-copper laminate composite. *Journal of Nuclear Materials*, 481:134–146, 2016.

[12] J. Reiser, M. Rieth, A.a Moeslang, H. Greuner, D.E.J. Armstrong, T. Denk, T. Gruening, W. Hering, A. Hoffmann, J. Hoffmann, H. Leiste, T. Mrotzek, R. Pippan, W. Schulmeyer, T. Weingaertner, and A. Zabernig. Tungsten (w) laminate pipes for innovative high temperature energy conversion systems. *Advanced Engineering Materials*, 17(4):491–501, 2014.

[13] M. Rieth, S.L. Dudarev, S.M. Gonzalez De Vicente, J. Aktaa, T. Ahlgren, S. Antusch, D.E.J. Armstrong, M. Balden, N. Baluc, M.-F. Barthe, W.W. Basuki, M. Battabyal, C.S. Becquart, D. Blagoeva, H. Boldyryeva, J. Brinkmann, M. Celino, L. Ciupinski, J.B. Correia, A. De Backer, C. Domain, E. Gaganidze, C. Garcia-Rosales, J. Gibson, M.R. Gilbert, S. Giusepponi,

B. Gludovatz, H. Greuner, K. Heinola, T. Hoeschen, A. Hoffmann, N. Holstein, F. Koch, W. Krauss, H. Li, S. Lindig, J. Linke, C. Linsmeier, P. Lopez-Ruiz, H. Maier, J. Matejicek, T.P. Mishra, M. Muhammed, A. Munoz, M. Muzyk, K. Nordlund, D. Nguyen-Manh, J. Opschoor, N. Ordas, T. Palacios, G. Pintsuk, R. Pippan, J. Reiser, J. Riesch, S.G. Roberts, L. Romaner, M. Rosinski, M. Sanchez, W. Schulmeyer, H. Traxler, A. Urena, J.G. Van Der Laan, L. Veleva, S. Wahlberg, M. Walter, T. Weber, T. Weitkamp, S. Wurster, M.A. Yar, J.H. You, and A. Zivelonghi. A brief summary of the progress on the EFDA tungsten materials program. *Journal of Nuclear Materials*, 442(1-3 SUPPL.1):173–180, 2013.

[14] M Fujitsuka, B Tsuchiya, I Mutoh, T Tanabe, and T Shikama. Effect of neutron irradiation on thermal diffusivity of tungsten–rhenium alloys. *Journal of Nuclear Materials*, 283-287:1148–1151, dec 2000.

[15] Na na Qiu, Yin Zhang, Cheng Zhang, Huan Tong, and Xi ping Song. Tensile properties of tungsten-rhenium wires with nanofibrous structure. *International Journal of Minerals, Metallurgy, and Materials*, 25(9):1055–1059, sep 2018.

[16] S. Antusch et al. Mechanical and microstructural investigations of tungsten and doped tungsten materials produced via powder injection molding. *Nuclear Materials and Energy*, 3-4:22–31, jul 2015.

[17] M Rieth, SL Dudarev, SM Gonzalez De Vicente, J Aktaa, T Ahlgren, S Antusch, DEJ Armstrong, M Balden, N Baluc, M-F Barthe, et al. Recent progress in research on tungsten materials for nuclear fusion applications in europe. *Journal of Nuclear Materials*, 432(1-3):482–500, 2013.

[18] J. Riesch, J.-Y. Buffiere, T. Hoeschen, M. di Michiel, M. Scheel, Ch. Linsmeier, and J.-H. You. In situ synchrotron tomography estimation of toughening effect by semi-ductile fibre reinforcement in a tungsten-fibre-reinforced tungsten composite system. *Acta Materialia*, 61(19):7060–7071, 2013.

[19] J Riesch, T Hoeschen, Ch Linsmeier, S Wurster, and J-H You. Enhanced toughness and stable crack propagation in a novel tungsten fibre-reinforced tungsten composite produced by chemical vapour infiltration. *Physica Scripta*, 2014(T159):014031, 2014.

[20] Yiran Mao, Jan Coenen, Sree Sistla, Chao Liu, Alexis Terra, Xiaoyue Tan, Johann Riesch, Till Hoeschen, Yucheng Wu, Christoph Broeckmann, and Christian Linsmeier. Design of tungsten fiber-reinforced tungsten composites with porous matrix. *Materials Science and Engineering: A*, 817:141361, jun 2021.

[21] Yiran Mao, Jan W. Coenen, Johann Riesch, Sree Sistla, Jürgen Almanstötter, Alexis Terra, Chang Chen, Yucheng Wu, Leonard Raumann, Till Höschen, Hanns Gietl, Rudolf Neu, Christoph Broeckmann, and Christian Linsmeier. Fiber volume fraction influence on randomly distributed short fiber tungsten fiber reinforced tungsten composites. *Advanced Engineering Materials*, mar 2020.

[22] Y Mao, J W Coenen, S Sistla, X Tan, J Riesch, L Raumann, D Schwalenberg, T Höschen, C Chen, Y Wu, C Broeckmann, and Ch Linsmeier. Development of tungsten fiber-reinforced tungsten with a porous matrix. *Physica Scripta*, T171:014030, jan 2020.

[23] Bruno Jasper, Jan W Coenen, Johann Riesch, Till Höschen, Martin Bram, and Christian Linsmeier. Powder metallurgical tungsten fiber-reinforced tungsten. *Materials Science Forum*, 825:125–133, 2015.

[24] B. Jasper, S. Schoenen, J. Du, T. Hoeschen, F. Koch, Ch. Linsmeier, R. Neu, J. Riesch, A. Terra, and J.W. Coenen. Behavior of tungsten fiber-reinforced tungsten based on single fiber push-out study. *Nuclear Materials and Energy*, 9:416–421, dec 2016.

[25] L. Raumann, J.W. Coenen, J. Riesch, Y. Mao, D. Schwalenberg, T. Wegener, H. Gietl, T. Höschen, Ch. Linsmeier, and O. Guillon. Modeling and experimental validation of a wf/w-fabrication by chemical vapor deposition and infiltration. *Nuclear Materials and Energy*, page 101048, jul 2021.

[26] Leonard Raumann, Jan Willem Coenen, Johann Riesch, Yiran Mao, Daniel Schwalenberg, Hanns Gietl, Christian Linsmeier, and Olivier Guillon. Improving the w coating uniformity by a

COMSOL model-based CVD parameter study for denser wf/w composites. *Metals*, 11(7):1089, jul 2021.

[27] L. Raumann, J.W. Coenen, J. Riesch, Y. Mao, H. Gietl, T. Höschen, Ch. Linsmeier, and O. Guillon. Modeling and validation of chemical vapor deposition of tungsten for tungsten fiber reinforced tungsten composites. *Surface and Coatings Technology*, 381:124745, jan 2020.

[28] J. Riesch, M. Aumann, J.W. Coenen, H. Gietl, G. Holzner, T. Hoeschen, P. Huber, M. Li, Ch. Linsmeier, and R. Neu. Chemically deposited tungsten fibre-reinforced tungsten – the way to a mock-up for divertor applications. *Nuclear Materials and Energy*, 9:75–83, may 2016.

[29] J.W. Coenen, Y. Mao, S. Sistla, A.v. Müller, G. Pintsuk, M. Wirtz, J. Riesch, T. Hoeschen, A. Terra, J.-H. You, H. Greuner, A. Kreter, Ch. Broeckmann, R. Neu, and Ch. Linsmeier. Materials development for new high heat-flux component mock-ups for DEMO. *Fusion Engineering and Design*, 146:1431–1436, feb 2019.

[30] H Gietl, A v Müller, JW Coenen, M Decius, D Ewert, T Höschen, Ph Huber, M Milwich, J Riesch, and R Neu. Textile preforms for tungsten fibre-reinforced composites. *Journal of Composite Materials*, 52(28):002199831877114, apr 2018.

[31] Y. Mao, J.W. Coenen, J. Riesch, S. Sistla, J. Almanstötter, B. Jasper, A. Terra, T. Höschen, H. Gietl, Ch. Linsmeier, and C. Broeckmann. Influence of the interface strength on the mechanical properties of discontinuous tungsten fiber-reinforced tungsten composites produced by field assisted sintering technology. *Composites Part A: Applied Science and Manufacturing*, 107:342–353, apr 2018.

[32] J Riesch, Y Han, J Almanstötter, JW Coenen, T Höschen, B Jasper, P Zhao, Ch Linsmeier, and R Neu. Development of tungsten fibre-reinforced tungsten composites towards their use in DEMO—potassium doped tungsten wire. *Physica Scripta*, T167(T167):014006, jan 2016.

[33] H Gietl, J Riesch, JW Coenen, T Höschen, Ch Linsmeier, and R Neu. Tensile deformation behavior of tungsten fibre-reinforced tungsten composite specimens in as-fabricated state. *Fusion Engineering and Design*, 124:396–400, mar 2017.

[34] Y Mao, J W Coenen, J Riesch, S Sistla, J Almanstötter, B Jasper, A Terra, T Höschen, H Gietl, M Bram, J Gonzalez-Julian, Ch Linsmeier, and C Broeckmann. Development and characterization of powder metallurgically produced discontinuous tungsten fiber reinforced tungsten composites. *Physica Scripta*, T170:014005, aug 2017.

[35] J.W. Coenen, J. Riesch, J-H You, M. Rieth, G. Pintsuk, H. Gietl, B. Jasper, F. Klein, A. Litnovsky, Y. Mao, et al. Advanced materials for a damage resilient divertor concept for DEMO: Powder-metallurgical tungsten-fibre reinforced tungsten. *Fusion Engineering and Design*, 124:964–968, dec 2017.

[36] Y Mao, J Engels, A Houben, M Rasinski, J Steffens, A Terra, Ch Linsmeier, and JW Coenen. The influence of annealing on yttrium oxide thin film deposited by reactive magnetron sputtering: Process and microstructure. *Nuclear Materials and Energy*, 10:1–8, jan 2017.

[37] J Riesch, J Almanstoetter, J W Coenen, M Fuhr, H Gietl, Y Han, T. Hoeschen, Ch Linsmeier, N Travitzky, P Zhao, and R Neu. Properties of drawn w wire used as high performance fibre in tungsten fibre-reinforced tungsten composite. *IOP Conference Series: Materials Science and Engineering*, 139:012043, jul 2016.

[38] J Riesch, A Feichtmayer, M Fuhr, J Almanstötter, J W Coenen, H Gietl, T Höschen, Ch Linsmeier, and R Neu. Tensile behaviour of drawn tungsten wire used in tungsten fibre-reinforced tungsten composites. *Physica Scripta*, T170:014032, oct 2017.

[39] J.W. Coenen, Y. Mao, S. Sistla, J. Riesch, T. Hoeschen, Ch. Broeckmann, R. Neu, and Ch. Linsmeier. Improved pseudo-ductile behavior of powder metallurgical tungsten short fiber-reinforced tungsten (wf / w). *Nuclear Materials and Energy*, 15:214–219, may 2018.

[40] A. v. Müller, M. Ilg, H. Gietl, T. Höschen, R. Neu, G. Pintsuk, J. Riesch, U. Siefken, and J.H. You. The effects of heat treatment at temperatures of 1100c to 1300c on the tensile properties of high-strength drawn tungsten fibres. *Nuclear Materials and Energy*, 16:163–167, aug 2018.

[41] H Bolt, V Barabash, G Federici, J Linke, A Loarte, J Roth, and K Sato. Plasma facing and

high heat flux materials - needs for ITER and beyond. *Journal of Nuclear Materials*, 307, Part 1(0):43–52, 2002.

[42] Xunxiang Hu, Takaaki Koyanagi, Makoto Fukuda, NAP Kiran Kumar, Lance L Snead, Brian D Wirth, and Yutai Katoh. Irradiation hardening of pure tungsten exposed to neutron irradiation. *Journal of Nuclear Materials*, 480:235–243, nov 2016.